Tribol Lett (2011) 41:345–351
DOI 10.1007/s11249-010-9712-3

ORIGINAL PAPER

Mechanism of Triboplasma Generation in Oil

Keiji Nakayama

Received: 14 July 2010 / Accepted: 6 October 2010 / Published online: 4 November 2010

Abstract The triboplasma that had been predicted in the rear clearance space of the sliding contact in oil was discovered by this author, who subsequently proposed that the triboplasma is generated through the discharge of air in the tribocharge electric field in the bubble. The proposed mechanism of triboplasma generation in oil has been studied in terms of the air in the bubble and the dissolved air in oil in the tribosystem of a diamond pin sliding on a sapphire disk in perfluoropolyether oil at atmospheric air pressure and in vacuum. The results of this study show that the triboplasma is not generated without bubble formation even if the oil contains air in the dissolved state. The air bubble grows over the entire gap of the rear divergent clearance space of the sliding contact so that the thickness of the oil film between the air bubble and the solid surfaces is negligibly small and the gap distance at which the triboplasma generation becomes greatest in the oil is the same as that in dry sliding. In other words, triboplasma is generated over the entire rear clearance gap of the sliding contact in the bubble in oil.

Keywords Triboplasma · Oil lubrication · Cavitations · Dissolved air · Perfluoropolyether · Tribocharging · Gas discharging · Triboluminescence · Photon emission

K. Nakayama (✉)
Advanced Research Institute, Chiba Institute of Technology, 2-17-1 Tsudanuma, Narashino, Chiba 275-0016, Japan
e-mail: keiji.nakayama@it-chiba.ac.jp

K. Nakayama
Nanotechnology Research Institute, AIST, 1-2-1 Namiki, Tsukuba, Ibaraki 305-8564, Japan

1 Introduction

Once flash temperature was observed in the 1940s [1], most tribological problems were analyzed and solved based on the rise in frictional temperature or frictional heat energy [2, 3]. However, there remain many tribological problems that can not be explained by the concept of thermodynamics based on frictional heat energy, which is closely associated with the state of aggregation of atoms, especially in the development of advanced technologies. This dilemma suggests that unknown high energetic states other than heat are generated at the sliding contact and its vicinity, such as energy related to electromagnetism and photons. In a search for this unknown energy source, this author has investigated systematically the triboemission of electrons, ions, and photons and concluded that a triboplasma should be generated around the sliding contact [4].

The predicted triboplasma was discovered with a circular shape in dry sliding in 2001 [5] and proven to be generated through discharging of the ambient air by the tribocharge-induced electric fields [6]. In 2006, the triboplasma was also discovered in oil, where it took on the shape of line along the frictional track [7]. This discovery may be important in terms of solving the various problems observed in machinery and machining under oil lubrication. The photon spectrum emitted from the triboplasma in oil also showed that the air discharge plasma is generated even under oil lubrication. As the line-shaped triboplasma was generated in the cavitation region, it was proposed that the triboplasma is generated by the discharge of air in a cavity or bubble formed in the oil. If this were to be the case, it would mean that triboplasma is generated in two steps: first, a cavity (or air bubble) is formed and, secondly, discharging of air occurs inside the bubble to generate the triboplasma.

In the study reported here, the mechanism of triboplasma generation in oil was investigated in terms of the air in the bubble and the dissolved state in oil. For this purpose, the experiments were performed for oil containing or not containing dissolved air at atmospheric pressure and in vacuum, respectively. The results show that triboplasma is not generated without bubble formation, even if the oil contains dissolved air and that the gap distance at which the triboplasma becomes most intense under oil lubrication is the same as that in dry sliding. They also show that triboplasma is generated over the entire rear clearance space in the bubble with an extremely thin oil film.

2 Experimental Procedure

Figure 1a, b show the apparatus used to measure the two-dimensional image and energy spectrum of photons emitted from the sliding contact and its vicinity while sliding a diamond pin with a tip radius of 300 μm on a rotating sapphire disk under dry sliding and oil-lubrication conditions. Figure 1c shows the apparatus used to measure the energy spectrum of photons emitted from the plasma generated by discharging oil between a steel needle electrode and a steel plate electrode, in which the electrode distance was approximately 300 μm.

Three kinds of two-dimensional photon images were measured, namely, the images of total, ultraviolet (UV), visible, and infrared (IR) photons. The designation "total" photon means that all photons were measured by the intensified CCD camera (ICCD camera), which detects photons in the wavelength region from 200 to 900 nm. In contrast, the UV, visible, and IR photons were measured separately by inserting an UV, a visible, or an IR optical filter between the optical microscope (OM) and the ICCD camera that allows passage of wavelengths of 290–420, 400–800, or 800–2,500 nm, respectively.

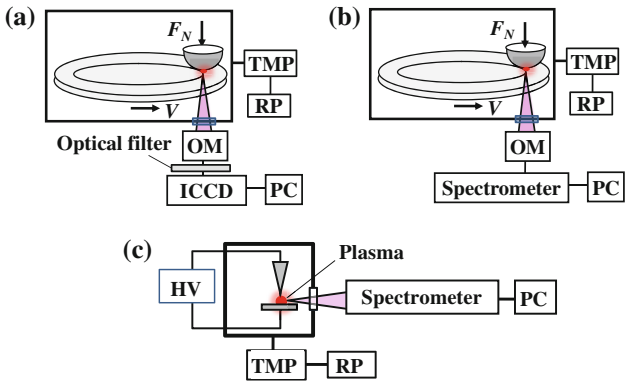

Fig. 1 Apparatuses used to measure two-dimensional image of tribo-photons (**a**), energy spectrum of tribo-photons (**b**), and energy spectrum of discharge photons (**c**). *OM* Optical microscope, *ICCD* intensified CCD camera, *PC* personal computer, *TMP* turbo-molecular pump, *RP* rotary pump, *HV* high voltage power supply, F_N normal force (mN)

The photon emission was measured while sliding a diamond pin with a tip radius of 300 μm on a sapphire (single crystal Al_2O_3) disk with a thickness of 1 mm and a diameter of 50 mm under perfluoropolyether (PFPE, Zdol 2000) oil lubrication. The viscosity and the average molecular weight of the PFPE oil was 85 × 10^{-6} m^2/s and 2000, respectively. The oil was coated on the sapphire disk as follows; first, the PFPE oil was dropped onto the disk surface, and then the oil-covered disk was fixed to a tribometer and the floating oil was removed by the centrifugal forces due to disk rotation at a rotational velocity of 1,000 rpm for 30 min. A meniscus was observed around the contact of the pin and the disk. All experiments were performed under a sliding velocity of $V = 32$ cm/s.

3 Results and Discussion

3.1 Air Bubble and Triboplasma

Figure 2 shows the two-dimensional image of the total photons emitted from the sliding contact and its vicinity while sliding a diamond pin with a tip radius $r = 300$ μm on a sapphire disk in PFPE oil (oil thickness 5 μm) under a normal force (F_N) of 490 mN and a sliding velocity of $V = 32$ cm/s. The color in the images shows the photon intensity distribution in the order red > yellow > green > blue > black = 0. The dotted line shows the frictional track and the arrow shows the direction of pin motion. Photons are seen to be emitted from two separate regions: the sliding contact and the rear outside of the contact. The photon emission region in the rear outside of contact is the triboplasma [7]. Namely, the plasma is generated along the frictional track, forming a shape of a straight-line [7], which is different from the ring-shape of the plasma generated under dry sliding [7].

The photons emitted from the triboplasma are composed of UV, visible, and IR photons [7] (see Fig. 7a below). Two-dimensional images of UV, visible, and IR photons were measured separately by inserting the optical filter into the measuring system under the PFPE oil-lubrication. These images are shown in Fig. 3. Figure 3a, b, and c shows the images displayed by camera in auto-contrast mode, in which the intensity of red is 34, 284, and 145 counts/pixel, respectively, where 1 pixel = 1.2 × 1.2 μm. Of these photon images, the UV image shows the triboplasma image itself, since the UV photons are emitted from the ionized plasma gas [7]. The UV image under oil-lubrication does not show the clear plasma line shape, but an elliptical shape. This should be due to the highly

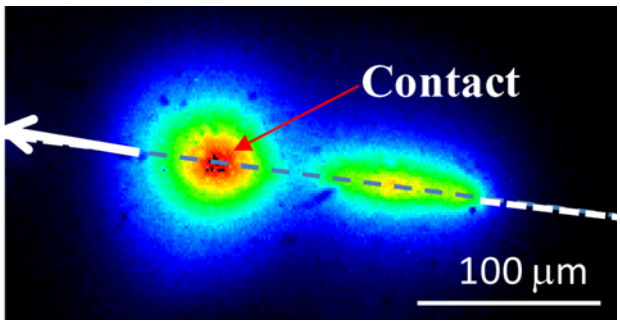

Fig. 2 Two-dimensional plane image of the total photons emitted from the sliding contact and its vicinity during sliding a diamond pin with $r = 300$ μm on a sapphire disk in perfluoropolyether (PFPE) oil with an average oil film thickness of 5 μm under $F_N = 490$ mN and velocity $(V) = 32$ cm/s. The figure is displayed with a camera auto-contrast mode. The exposure time of the ICCD camera was 5 min. The *color* shows the intensity in the order of *red* (=467 counts/pixel) > *yellow* > *green* > *blue* > *black* = 0. The *arrow* shows the direction of pin sliding

scattering nature of UV photons with a short wavelength [7]. The visible photon emission intensity is too strong at the sliding contact to see the weak plasma image, whereas the IR image clearly gives two separated photon emission regions at the contact and plasma regions, respectively. The shape of the latter shows a clear line-shaped plasma image due to the low scattering nature of IR photons with a long wavelength [7].

To highlight the plasma image of the visible photon in Fig. 3b, the red level in Fig. 3b was lowered from 284 to 32 counts/pixel to give Fig. 3e. For comparison, the red level in Fig. 3a and 3c was also lowered from 34 to 7 and from 145 to 32 counts/pixel, respectively, to give Fig. 3d and 3f. The black zone in Fig. 3d–f shows the region where the photon intensity is beyond the red level. Thus, the plasma line shape is clearly detectable in the visible image in Fig. 3e. That the images are larger in Fig. 3d–f than in the corresponding images in Fig. 3a–c should be the results of photon scattering.

Figure 4a–c shows the two-dimensional images of the UV, visible, and IR photons shown in Fig. 3a, e, f and the photon intensity profiles along the frictional track. The UV image shows that the distance between the center of the sliding contact and center of the plasma (l_o) is 90 μm, as shown in Fig. 4a. In contrast, the photon intensity profile in the plasma region in the visible image shows a plateau, as seen in Fig. 4b, so that the distance l_o, is not clear. On the other hand, the IR photon intensity profile gave $l_o = 90$ μm, although the peak has some second sharp peaks at the top. In the contact geometry of a sphere with r = 300 μm on a plate, the distance $l_o = 90$ μm corresponds to a clearance gap distance (d_o) of 14 μm. Namely, the triboplasma becomes most intense at the gap distance of $d_o = 14$ μm under oil-lubrication. In the UV and IR photon images in Fig. 4a and 4c, a small peak appeared in front of the sliding contact, although it is difficult to see it in the visible image. The origin of the front peak is not clear.

For comparison, two-dimensional images of UV, visible, and IR photons and the photon intensity profiles along the frictional track were measured under sliding in dry air under the same experimental conditions as those measured in the PFPE oil-lubrication in Fig. 3a–c. These images are

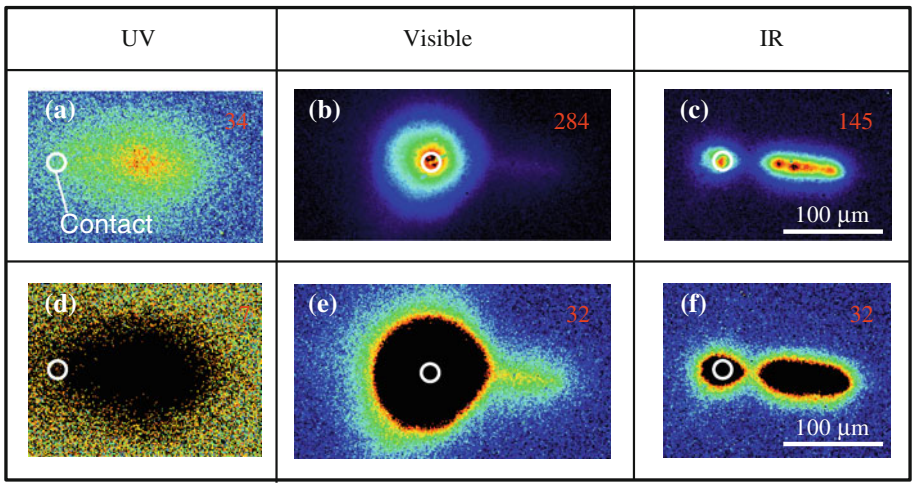

Fig. 3 Two-dimensional images of ultraviolet (*UV*), visible, and infrared (*IR*) photons emitted from the sliding contact and its vicinity during sliding a diamond pin with $r = 300$ μm on a sapphire disk in PFPE oil with the average oil film thickness 5 μm under $F_N = 490$ mN and $V = 32$ cm/s. **a**, **b**, **c** Images displayed with a camera auto-contrast mode, with intensities at the *red* of 34, 284, and 145 counts/pixel for UV (**a**), visible (**b**), and IR (**c**) photon image, respectively. d, e, f *Black* zone surrounded by *red* shows the photon intensity beyond the intensity at the *red* color, with intensities of 7, 32 and 32 counts/pixel in the UV (**d**), visible (**e**), and IR (**f**) range, respectively. *White circle* Theoretical Herzian contact area with a radius $r = 8$ μm

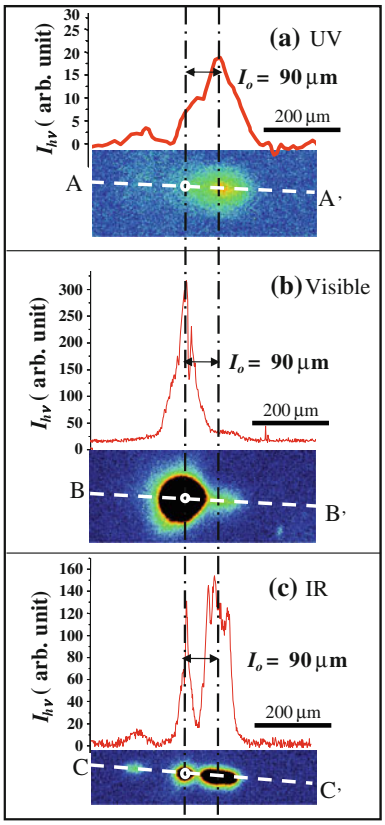

Fig. 4 Two-dimensional images and intensity profiles of UV, visible, and IR photons emitted from the sliding contact and the vicinity during sliding a diamond pin with $r = 300$ μm on a sapphire disk in PFPE oil under $F_N = 490$ mN and $V = 32$ cm/s. l_o Distance between the center of the sliding contact and center of the plasma. The intensity profiles were measured along the frictional track shown by A–A′, B–B′, C–C′ and D–D′

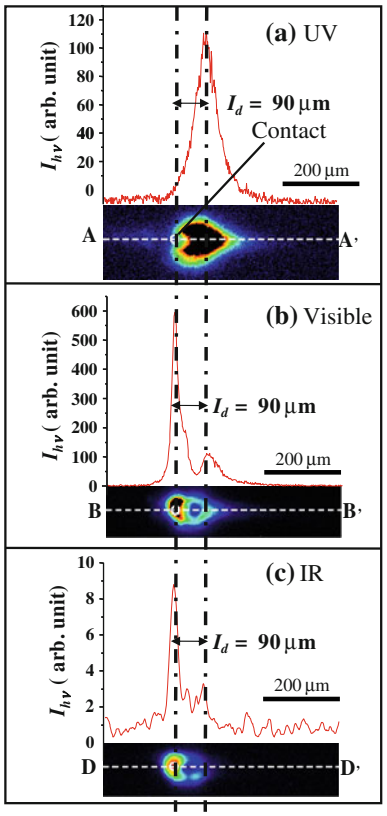

Fig. 5 Two-dimensional images and intensity profiles of UV, visible, and IR photons emitted from the sliding contact and the vicinity during sliding a diamond pin with $r = 300$ μm on a sapphire disk under dry sliding in dry air under $F_N = 490$ mN and $V = 32$ cm/s. *Red* shows 40 (**a**), 275 (**b**), and 196 (**c**) counts/pixel. l_d Distance between the center of the sliding contact and that of the plasma. The intensity profiles were measured along the frictional track shown by A–A′, B–B′, C–C′ and D–D′

shown in Fig. 5a–c, where Fig. 5a and 5b are the contrast-modified images and Fig. 5c is the auto-contrast image. These figures clearly show the ring-shaped plasma image. In dry sliding, the UV photon intensity is extremely weak at the sliding contact and greatest at the crossing point of the triboplasma ring and the frictional track, i.e., at the center of the plasma. The distance between the center of the sliding contact and that of the plasma (l_d) was 90 μm, which is equal to $l_o = 90$ μm in the oil-lubrication. On the contrary, the visible and IR photon emission intensity can be seen to be relatively weak in the plasma region and strongest at the sliding contact. In the visible photon image, the plasma ring is also clearly displayed to give $l_d = 90$ μm. In the IR photon image, the photon intensity profile was noisy, but it also gave $l_d = 90$ μm. The distance $l_d = 90$ μm corresponds to the gap distance of 14 μm described above. Namely, the triboplasma is generated at the same clearance gap distance of 14 μm in both the dry and oil-lubricated sliding. Thus, based on these results, it can be concluded that the air bubble is formed over the entire clearance and that the air pressure inside the bubbles is the same value as that of the ambient atmospheric air pressure. This conclusion is coincident with published results [8–10]. These results mean that triboplasma is generated over the entire clearance space even in oil.

3.2 Effect of Air Pressure on Triboplasma Generation

In order to understand how air in the oil affects the plasma generation, two-dimensional images and the energy spectra of photons were investigated under the atmospheric air pressure and in vacuum.

Figure 6a–c show the two-dimensional images of UV, visible, and IR photons emitted under PFPE oil-lubrication while sliding a diamond pin with r = 300 μm on a sapphire disk under $F_N = 490$ mN, $V = 32$ cm/s and an atmospheric pressure of $(p) = 1 \times 10^5$ Pa. The UV photon plasma image can be seen to be widely spread to give almost circular shape, as seen in Fig. 7a, whereas the plasma line image is not seen in the visible and IR photons due to the high photon intensity with high scattering at the

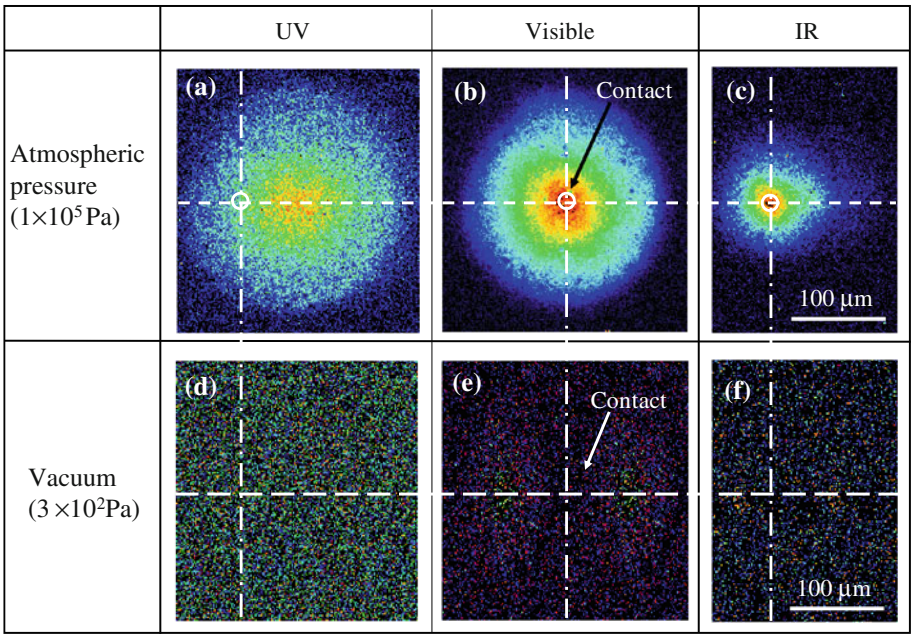

Fig. 6 Two-dimensional images of UV, visible, and IR photons emitted under PFPE oil lubrication with the film thickness $r = 13$ μm at atmospheric pressure $(p) = 1 \times 10^5$ Pa (**a**) and after evacuating the dissolved air in the PFPE oil under $p = 3 \times 10^2$ Pa (**b**) under $F_N = 490$ mN and $V = 32$ cm/s. The figures are displayed with a camera auto-contrast mode

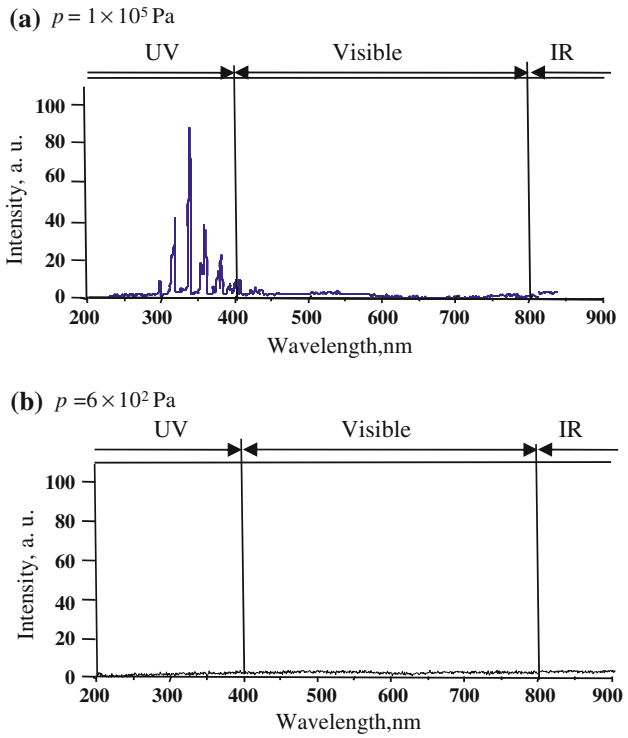

Fig. 7 Energy spectrum of photons emitted from the sliding contact and the vicinity during sliding a diamond pin with $r = 300$ μm on a sapphire disk in PFPE oil under $F_N = 980$ mN and $V = 32$ cm/s at atmospheric pressure $p = 1 \times 10^5$ Pa (**a**) and after evacuating the dissolved air in the PFPE oil under $p = 6 \times 10^2$ Pa (**b**)

sliding contact, as seen in Fig. 7b and 7c. The high scattering of the photons under oil-lubrication is probably due to the thick oil film of 13 μm in this experiment. On the other hand, Fig. 6d–f shows the two-dimensional photon images measured after evacuating the dissolved air from the PFPE oil at $p = 3 \times 10^2$ Pa. Here, it can be clearly seen that the UV photon image has completely disappeared in the oil in vacuum. This plasma disappearance in vacuum under oil-lubrication corresponds to the plasma disappearance in dry sliding in vacuum at $p = 10^1$–10^2 Pa [11]. Namely, the air was insufficient not only for the bubble formation but also for air discharging itself to produce triboplasma. In other words, by removing the dissolved air, we can prevent triboplasma generation under oil-lubrication. It is noted that the visible and IR photons almost disappeared at the sliding contact. This is a surprising observation since it suggests that the photons are emitted from the air molecules in the oil compressed under the Hertzian pressure. Just how the air molecules were excited to emit photons in the compressed oil requires further investigation.

Figure 7a and 7b show the photon energy spectrum measured under PFPE oil-lubrication at the atmospheric air pressure $p = 1 \times 10^5$ Pa and after evacuating the dissolved air from the oil at the air pressure of $p = 6 \times 10^2$ Pa, respectively. Many narrow bands can be seen to originate from the air discharge plasma, and these are clearly seen in the UV region under the atmospheric pressure [7]. These narrow bands have completely disappeared in the spectrum after removing the air from the oil, as seen in Fig. 7b, clearly proving that triboplasma cannot be generated without air in oil.

These results demonstrate that triboplasma is generated by discharging of air in the bubble, i.e., in the gas phase. However, it is not clear what happens to the air in the dissolved state? To answer this question, the energy spectrum of photons were measured during the discharge of the oils without and with dissolved air between the steel needle

and steel plate electrodes. The distance between the electrodes was about 300 μm. Figure 8a shows the energy spectrum of photons emitted during discharging of the PFPE oil containing dissolved air under the atmospheric pressure $p = 1 \times 10^5$ Pa and an applied voltage of 1.6 kV between the electrodes. This spectrum is completely different from that under the oil-lubrication at $p = 1 \times 10^5$ Pa in Fig. 7a. Namely, it has no narrow bands due to the air discharge. Just after the experiment in Fig. 8a, the same oil was evacuated to remove the dissolved air at $p = 6 \times 10^2$ Pa, and then the discharge experiment was performed under the applied voltage ranged from 0.7 to 1.3 kV between the electrodes to give the photon energy spectrum shown in Fig. 8b. As the dissolved air was removed from the oil, the spectrum in Fig. 8b must be the PFPE oil discharge spectrum itself. It is noted that the spectra of the photon energy from the oil with and without dissolved air are almost identical, leading to the conclusion that triboplasma cannot be generated without air bubble formation, even if the air is contained in oil in the dissolved state.

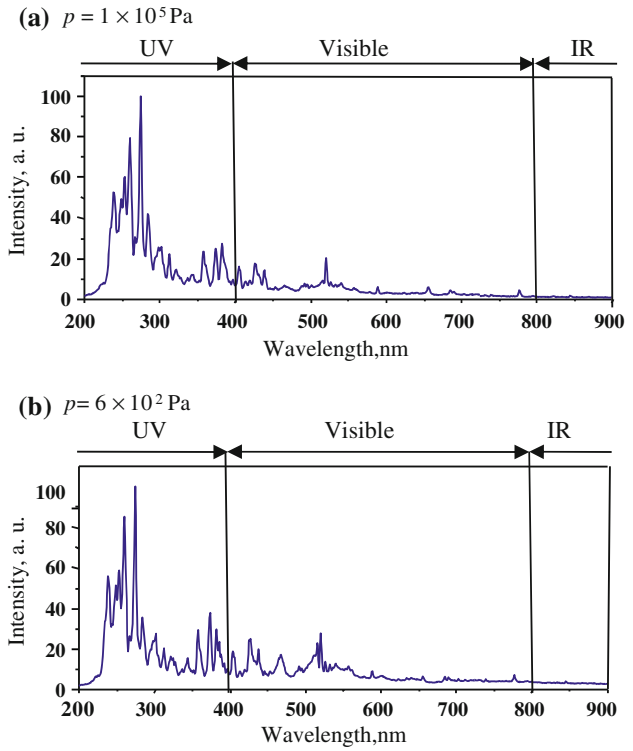

Fig. 8 Energy spectrum of photons emitted during discharging of PFPE oil between a steel needle and a flat surface of steel disk under the applied voltage 1.6 kV at an atmospheric pressure $p = 1 \times 10^5$ Pa (**a**) and after evacuating the dissolved air in the PFPE oil under an applied voltage of 0.3–1.3 V at $p = 6 \times 10^2$ Pa (**b**)

3.3 Mechanism of Triboplasma Generation in Oil

A model of triboplasma generation in oil is depicted in Fig. 9 based on the experimental findings and discussions of these. It is well-known that cavitation occurs in the rear divergent clearance space of the sliding contact, where the oil pressure is extremely reduced [8]. Some of the dissolved air in the oil is liberated from the oil phase into the cavity [12], or the ambient outside air enters into the oil film through the clearance to form bubbles [9]. These bubbles are then filled with the air expanding toward the entire gap distance between the sphere and the disk. The air pressure in the bubble is almost the same as that in the ambient atmospheric pressure [8].

On the other hand, several mechanisms on tribocharging or triboelectrification have been proposed to date. These are largely classified into three kinds of mechanisms, i.e., solid–solid contact [13], solid–liquid contact [14], and electric double layer [15]. However, it is not clear whether, under the present experimental conditions, these tribocharging mechanisms act simultaneously or whether one of these predominates to cause the intense electric fields inside the bubble. The electrons emitted from the negatively charged friction track surface enter into the bubble, passing through the oil film, and then accelerate together with the stray electrons existing in the oil film and air in the bubble to cause the air-discharging. Through the electron avalanche process in discharge, huge numbers of electrons and positive ions are produced to generate the triboplasma. The electron avalanche process reaches its maximum at the gap distance corresponding to the electrode distance d at the minimum point in the *V-pd* relationship in *Paschen's law* [16], where V is the spark voltage, p is the gas pressure, and d is the electrode distance, respectively. The electrode

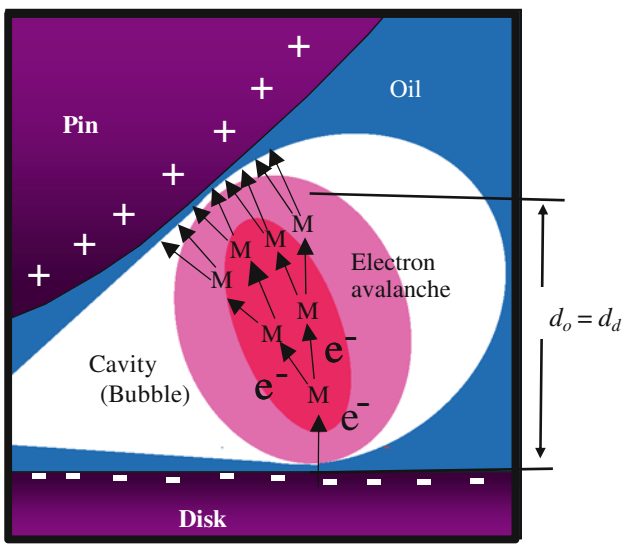

Fig. 9 Model of triboplasma generation in oil

distance corresponds to the clearance gap distance $d_o = 14$ μm in the oil-lubrication condition and $d_o = 14$ μm in the dry sliding. This correspondence $d_o = d_d$ means that the oil film thickness between the air bubble and the surfaces of the diamond pin and the sapphire disk are negligibly small compared to the gap distance 14 μm, as seen in Fig. 9.

When the air pressure in the cavity is reduced to the extremely low level in the divergent region of the sliding contact, the oil itself evaporates to produce a cavity filled with the evaporated gaseous oil molecules, and then sonoluminescence photons are emitted [17]. However, as the PFPE oil used in the present study has an average molecular weight of 2,000, the sliding condition seems to be too low to cause such intense reduced pressure. Further, the energy spectrum in the UV region of photons emitted under PFPE oil lubrication showed air discharge plasma and the plasma luminescence disappeared after degassing of the air. These facts show that the present luminescence does not have a sonoluminescence origin, but is due to the air discharge origin.

Namely, as stated above, triboplasma under oil lubrication is generated through two stages. First, an air bubble is formed in the rear clearance gap of the sliding contact, followed by air-discharging inside the bubble due to the intense electric field caused by tribocharging to generate triboplasma. As the mechanism of the triboplasma generation under oil lubrication has been clarified, the triboplasma will be one of the essential technological factors in the reduction of friction and wear, prevention of oil degradation, and development of new type of lubricant additives under oil lubrication.

4 Conclusions

The results of this study confirm the previously proposed mechanism of triboplasma generation under oil lubrication, namely, that it is due to a two-stage mechanism: cavities or air bubbles are first formed in the divergent clearance space of the rear part of the sliding contact followed by the discharge of air inside the bubble due to the intense tribocharge-electric field, thereby generating a triboplasma. The bubble expands over the entire gap, so that the thickness of the oil film between the air bubble and the sliding surfaces are negligibly small, and the air pressure inside the bubble is almost equal to the ambient atmospheric pressure; consequently, the gap distance at which plasma generation becomes most intense under oil-lubrication is almost equal to that in dry sliding—namely, triboplasma spread over the entire clearance space even in oil. As bubble formation is essential to the generation of a triboplasma, the generation of the triboplasma can be prevented by removing the air from the oil. It was also found that photons emitted from the sliding contact almost disappear when air is removed from the oil. However, the mechanism of photon emission originated from the air in the sliding contact is not clear and requires further study.

Acknowledgments This work was supported by the KAKENHI (Grant-in-Aid for Scientific Research (A), 20246035).

References

1. Bowden, F.P., Stone, M.A., Tudor, G.T.: Hot spot on rubbing surfaces and the denotation of explosives by friction. Proc. R. Soc. A **188**, 329–349 (1947)
2. Sakurai, T., Sato, H.: Study of Corrosivity and correlation between chemical reactivity and local carrying capacity of oils containing extreme pressure agents. ASLE Trans. **9**, 77–87 (1966)
3. Archard, J.F.: The temperature of rubbing surfaces. Wear **2**, 438–455 (1958/1959)
4. Nakayama, K.: Tribophysical phenomena and tribochemical reaction. Jpn. J. Tribol. **42**, 1077–1084 (1997)
5. Nakayama, K., Nevshupa, R.A.: Plasma generation in a gap around a sliding contact. J. Phys. D Appl. Phys. **35**, L53–L56 (2002)
6. Nakayama, K., Nevshupa, R.A.: Characteristics and pattern of plasma generated at sliding contact. Trans. ASME: J. Tribol. **125**, 780–787 (2003)
7. Nakayama, K.: The plasma generated and photons emitted in an oil-lubricated sliding contact. J. Phys. D Appl. Phys. **40**, 1103–1107 (2007)
8. Dowson, D., Higginson, G.R.: Elastohydrodynamic Lubrication, p. 35. Pergamum, Oxford (1997)
9. Kaneta, M., Wang, J., Hahimoto, T., Wakamizu, Y., Nishikawa, H.: Effect of oil starvation on point contact EHL films in short stroke reciprocating motion. *Proc. Int. Tribo. Conf. Austrib 2006*, No. 222 (2006)
10. Wedeven, L.D., Evans, D., Cameron, A.: Optical analysis of ball bearing starvation. Trans. ASME: J. Lub. Tribol. **93**, 349 (1971)
11. Nakayama, K., Nevshupa, R.: Effect of dry air pressure on characteristics and patterns of tribomicroplasma. Vacuum **74**, 11–17 (2004)
12. Schweizer, P.H., Szebehely, V.G.: Gas evolution in liquid and cavitation. J. Appl. Phys. **21**, 1218 (1950)
13. Harper, W.R.: Contact and Frictional Electrification, p. 50. Oxford, Clarendon press (1967)
14. Phair, B., Bensch, L., Duchowsky, J., Khazan, M., Tsalyuk, V.: Overcoming the electrostatic discharge in hydraulic, lubricating and fuel-filtration applications by incorporating novel synthetic filter media. Tribol. Trans. **48**, 343–351 (2005)
15. Harvey, T.J., Wood, R.J.K., Denuault, G., Powrie, H.E.G.: Investigation of electrostatic charging mechanisms in oil lubricated tribo-contacts. Tribol. Int. **35**, 605–614 (2002)
16. Engel, A.: Ionized Gases, p. 196. AOP Press, New York (1993)
17. Moran, M.J., Lowry, R.E., Sweider, D.R.: Observation of single-pulse sonoluminescence. Nucl. Instrum. Methods **B96**, 651–657 (1995)